

F-3-5L

Detailed Balance in Quasi-Ballistic Electron Transport under Nanoscale Device Structures

Hiroyuki Kusaka and Nobuyuki Sano

Institute of Applied Physics, University of Tsukuba, Tsukuba, Ibaraki 305-8573, JAPAN
Phone/Fax: +81-29-853-6465, E-mail: kusaka@hermes.esys.tsukuba.ac.jp

1. Introduction

The channel length of the most advanced Si-MOSFETs is now scaled below 10 nm regimes [1]. This is even smaller than a typical mean-free path in semiconductor devices at room temperature. As a result, it is conjectured that the device properties might be evaluated by neglecting scatterings and assuming nearly ballistic transport, as illustrated in Fig.1 [2]. On the other hand, it has been theoretically shown that scatterings cannot be neglected even in nano-scale channels [3]. In the present paper, we investigate the detailed-balance of electron transport via Monte Carlo (MC) simulations and demonstrate explicitly that the picture of electron transport is much more involved than the naive ballistic picture.

2. Device Structure and Simulation Method

Figure 2(a) shows the device structure, one dimensional *n-i-n* diode consisting of the slab (denoted as channel) sandwiched with highly doped regions (denoted as S region and D regions), used in this study. The length of the S and the D regions is 100 nm and the channel length is either 10 nm or 50 nm. The periodic boundary conditions are imposed. The doping density of the S and D regions is 10^{20} cm⁻³, whereas the channel is intrinsic. The electric potential, as shown in Fig.2(b) and (c) for 10 nm and 50 nm devices, are obtained from the Drift-Diffusion simulations and the MC simulations are performed under these potentials.

3. Results and Discussion

Figure 3(a) shows the velocity distributions at various locations along the channel and those at the bottleneck obtained from the MC simulations by artificially changing the phonon energies are shown in Fig.3(b). Since the dashed line shows the distribution function with no scattering in the channel (ballistic), the difference between the solid and dashed lines result from the scatterings taking place in the channel. Notice that the negative velocity distribution grows as the phonon energy is decreased. Since the scattering rate for phonon absorption is directly proportional to the number of excited phonons, in contrary to the one for phonon emission, and the number of phonons increases as the phonon energy decreases, this implies that the phonon-absorption processes may play an important role in analyzing quasi-ballistic transport. This is indeed the case; we have investigated the number of scatterings for absorption and emission at various positions along the channel for $L = 10$ and 50 nm. The results are shown in Figs. 4(a) and (b). We would like to stress that the results in both cases show very similar trends; the number of absorption scatterings is nearly equal to that of emission around the top of the potential barrier in the channel, whereas the emission processes dominate over the absorption near the drain in the channel, as we expect under highly nonequilibrium situations. Almost the same contribution of the absorption and emission events around the bottleneck region is interpreted as the detailed balance and, thus, the local equilibrium condition being realized. Notice that the detailed balance indeed strictly holds true in the S and D regions, as shown in the inset. A snapshot of

electrons' population in real space under steady state is shown in Fig. 5. It is observed that there are many electrons with low kinetic energy around the bottleneck. These electrons are responsible to mainly the absorption processes and lead to the detailed balance. These results imply that even if the devices become in the nano-scale regime, electrons around the bottleneck are in the local equilibrium states.

This scenario is further confirmed by directly evaluating the detailed balance due to scattering processes. The detailed balance implies that the collision integral (right-hand side) of the Boltzmann Transport Equation exactly vanishes for every wave-vector \mathbf{k} and Figs.6 and 7 depict the meaning of the detailed balance. Because of the limited computational power, the contribution of the in-scattering and the out-scattering terms in the collision integral cannot be evaluated for every \mathbf{k} . In the present study, they are integrated over the angles (θ and ϕ) and, thus, we consider the balance of the in- and out-scattering contributions for every $|\mathbf{k}|$, instead of \mathbf{k} . Figures 8 (a) and (b) show thus obtained the in- and out-scattering as a function of $|\mathbf{k}|$ at the bottleneck and at the middle point of the potential drop, respectively. It should be noted that the in- and out-scattering contributions around the bottleneck are almost identical at every $|\mathbf{k}|$ and the detailed balance is indeed satisfied. On the other hand, their contributions deviate greatly at the middle point of potential drop and represent that the electrons there are highly nonequilibrium. Figure 9 shows the in- and out-scattering at various locations along channel. The transition of local equilibrium regions to highly nonequilibrium (quasi-ballistic) regions is clearly seen and, thus, electron transport under nano-scale structures is much more involved than the simple ballistic picture. These results substantiate our claim: electrons around the bottleneck are in local equilibrium and their transport is a mixture of diffusive and quasi-ballistic.

The present finding is very important from the viewpoint of quantum transport. At present, most calculations based on quantum transport such as the Nonequilibrium Green Functions (NEGF) assume the coherent transport and the scattering is treated as a minor effect due to *pre-assumed* ballistic transport. However, the present results suggest that the phase coherence might be destroyed by scatterings around the bottleneck region and electron transport might be intrinsically incoherent.

4. Conclusions

We have carried out 3D many-particle Monte Carlo simulations under nano-scale structure, and we have found that the detailed balance holds around the bottleneck region. It implies that electrons around the bottleneck are in local equilibrium and carrier transport for low energy electrons is diffusive, in contrary to the previous conjectures.

References

- [1] H. Wakabayashi, et al., in IEDM Tech Dig. (2003) pp.989-991.
- [2] F. Assad, et al., IEEE Trans. Electron Devices vol.47 (2000) pp.232-240.
- [3] N. Sano, Phys. Rev. Lett **93** (2004) 246803

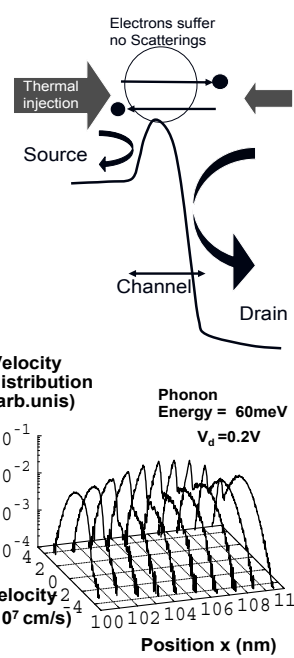
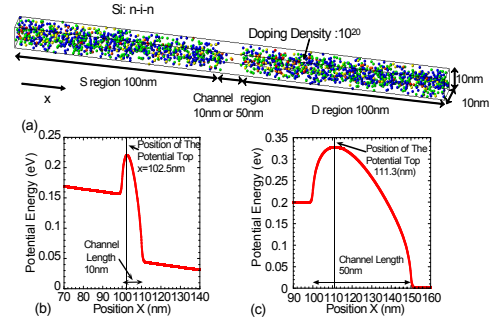


Fig. 1 (Left) Schematic drawing of purely ballistic transport under nanostructures. No scattering takes place in the channel

Fig. 2 (Right) (a) n-i-n structure used for simulation in this study. The applied bias is 0.2V. The doping density is assumed to be $10^{20} / \text{cm}^3$ in S-region and D-region. The periodic boundary condition is appended at all boundaries. (b) and (c) show the potential profiles derived from the Drift-Diffusion simulations along the channel with 10nm and 50nm respectively.



The figure is a 3D surface plot showing the velocity distribution as a function of position x (in nm) and velocity (in units of 10^7 cm/s). The vertical axis represents the velocity distribution in arbitrary units, ranging from 10^{-4} to 10^{-1} . The horizontal axis represents position x in nm, with labels at $10^6, 10^7, 10^8, 10^9, 10^{10}, 10^{11}$. The depth axis represents velocity in 10^7 cm/s , with labels at 0, 2, 4. The surface exhibits periodic oscillations in both the position and velocity directions, with a central peak at approximately $x = 10^7 \text{ nm}$ and $v = 2 \times 10^7 \text{ cm/s}$.

(a) (b)
Fig. 3 (a) Velocity distributions at different locations along the channel (b) Velocity distribution functions at the bottleneck by varying the phonon energies in the channel. The negative velocity distribution grows as the phonon energy is decreased, due to the increase of phonon absorption processes

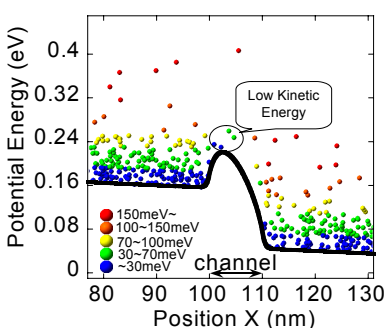


Fig. 5 Snapshot of the electron distribution in real space under steady state. The solid line shows the electronic potential energy.

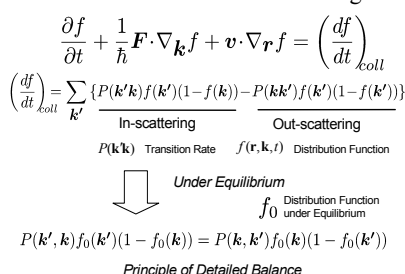


Fig. 6 Boltzmann Transport Equation and its collision integral. The detailed balance holds for every wave vector \mathbf{k} and \mathbf{k}' under thermal equilibrium, so that the probability of in-scattering and out-scattering becomes the same.

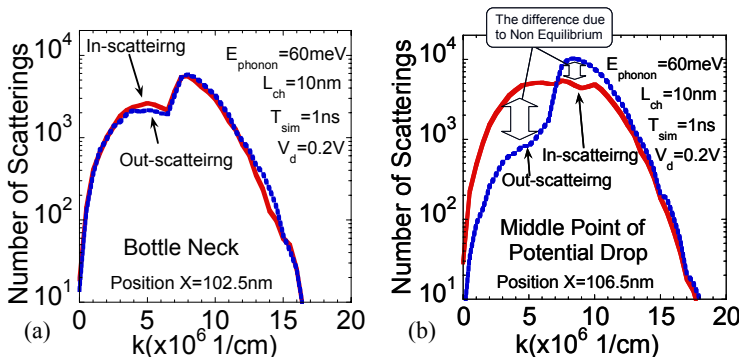
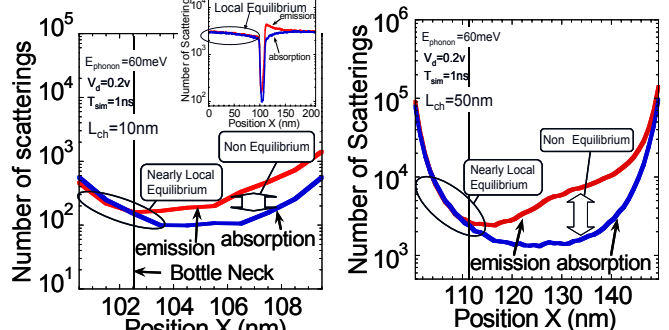


Fig. 8 Number of in-scatterings and out-scatterings as a function of $|k|$ at (a) bottleneck and (b) middle point of the potential drop respectively. The channel length is 10nm.



(a) (b)
Fig. 4 (a) Number of absorption and emission processes at each position in the channel. The phonon energy is 60meV. The channel length is 10nm. Inset shows the number of scatterings at each position in all device regions. (b) The number of scatterings at each position with the channel length of 50nm.

$$\int d\theta \int dk' f(r, k, t) = \int d\theta \int dk' f(r, k', t)$$

Fig. 7 (a) Schematic drawing of in-scatterings and out-scatterings integrated over angles in k -space. Dashed and dotted arrows imply in-scatterings to $|k|$ and out-scatterings from $|k|$, respectively. The amount of in-scatterings and out-scatterings which are integrated over angles are the same under equilibrium, since the magnitude of each dashed arrows is the same with that of dotted counterparts leading to the detailed balance.

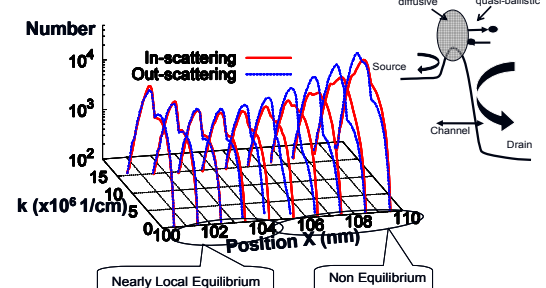


Fig. 9 Number of in-scatterings and out-scatterings as a function of $|k|$ at each position. Electrons are in nearly local equilibrium in the region around the bottleneck, whereas electrons are highly nonequilibrium near the D-region.